JACS
JOURNAL OF THE AMERICAN CHEMICAL SOCIETY
Article
pubs.acs.org/JACS

Solid-State MAS NMR Studies of Brønsted Acid Sites in Zeolite H-Mordenite

Hua Huo,[†,∥] Luming Peng,[‡] Zhehong Gan,[§] and Clare P. Grey*[,†,∥]

[†]Department of Chemistry, State University of New York at Stony Brook, Stony Brook, New York 11794-3400, United States
[‡]Key Laboratory of Mesoscopic Chemistry of MOE, School of Chemistry and Chemical Engineering, Nanjing University, Nanjing 210093, China
[§]National High Magnetic Field Laboratory, 1800 East Paul Dirac Drive, Tallahassee, Florida 32310, United States
[∥]Department of Chemistry, University of Cambridge, Lensfield Road, Cambridge CB2 1EW, United Kingdom

ABSTRACT: $^{17}O-^{1}H$ double resonance NMR spectroscopy was used to study the local structure of zeolite H-Mordenite. Different contact times were used in cross-polarization magic angle spinning (CPMAS) NMR, CP rotational-echo double resonance (CP-REDOR) NMR, and heteronuclear correlation (HETCOR) NMR spectroscopy to distinguish between Brønsted acid sites with different O−H distances. The accessibility of the various Brønsted acid sites was quantified by adsorbing the basic probe molecule trimethylphosphine in known amounts. On the basis of these experiments, locations of different Brønsted acid sites in H-Mordenite (H-MOR) were proposed. The use of ^{17}O chemical shift correlations to help assign sites is discussed.

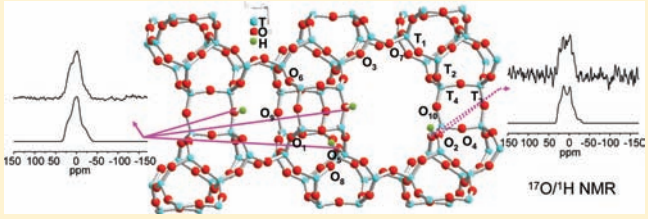

INTRODUCTION

Mordenite (MOR)-type zeolites are important catalysts for many industrial applications. The acidic form, H-Mordenite, in particular, shows spectacular selectivity for, for example, the selective transalkylation and disproportionation of alkylbenzenes.[1,2] This selectivity mainly lies in the availability of the catalytically active sites, Brønsted acid sites in acid-catalyzed reactions, which are located in the cavities with specific shape and scale and only allow reactants with suitable sizes and geometries to enter.[3] A determination of the locations of Brønsted acid sites in acidic zeolites is essential if structure−reactivity relationships are to be developed.

The structure of a mordenite-type zeolite is shown in Figure 1. There are four crystallographically nonequivalent tetrahedral cation sites (T_1-T_4) and 10 framework oxygen sites (O_1-O_{10}). The main channels, circumscribed by 12-rings, are along the *c* axis, measuring 6.5 × 7.0 Å. The smaller 8-ring channels lie parallel to the main channels, measuring 2.6 × 5.7 Å. The third type of cavity in mordenite is along the *b* direction, circumscribed by 8-rings, measuring 3.4 × 4.8 Å. This cavity is often referred to as the "side pocket" and connects the 12-ring channel with the 8-ring channel through 8-rings.

The location of protons in H-MOR has been extensively studied by a variety of methods, including X-ray/neutron diffraction, FTIR spectroscopy, and ab initio calculations; however, conflicting results have been reported, and their location is still under debate. Early X-ray diffraction studies on dehydrated H-MOR by Mortier and co-workers concluded that the probability of proton attachment to the different oxygen sites was equal.[4] Martucci et al. studied the deuterated zeolite mordenite by neutron diffraction and claimed that there are

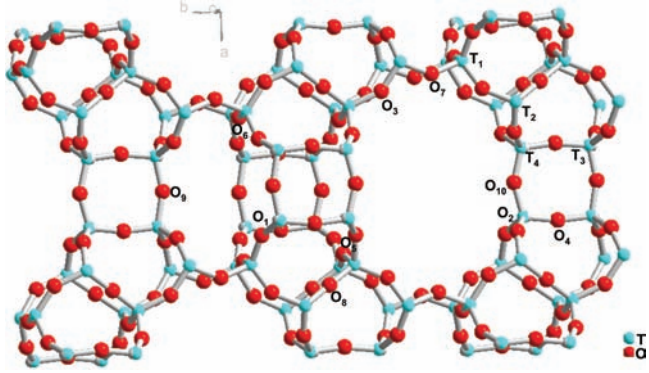

Figure 1. The structure of mordenite type zeolites, showing the main channel along the *c* axis circumscribed by 12-rings.

four different Brønsted acid sites. One is on the framework oxygen O_6, at the entrance of the side pocket; another is on O_9, in the center of the 8-ring channel; the other two are on O_5 and O_{10}, pointing into the center of the 12-ring.[5] On the basis of FTIR studies of zeolites H-MOR loaded with probe molecules, the low frequency and high frequency ν(OH) bands have been assigned to OH groups in the 8-ring and 12-ring main channel, respectively.[6] Bevilacqua and co-workers further proposed that the low frequency OH group corresponds to the O_6 site, while the high frequency OH groups are due to Brønsted acid sites at O_2, O_5, O_3, O_7, and O_{10}.[7,8] Marie et al. reported that there is a

Received: February 28, 2012
Published: May 3, 2012

© 2012 American Chemical Society

dx.doi.org/10.1021/ja301963e | *J. Am. Chem. Soc.* 2012, 134, 9708−9720

third type of Brønsted acid site corresponding to a ν(OH) band at an intermediate frequency and suggested there are three types of OH groups located at $O_2-O_7-O_9$.[9] Ab initio density function theory (DFT) calculations of zeolites H-MOR gave similar results, namely that the Brønsted acid sites are located at either the $O_2-O_7-O_9$[10] or $O_2-O_7-O_9-O_{10}$[10,11] positions. Alberti conducted a cross-check of crystallochemical and spectroscopic data and concluded that the most likely sites for the Brønsted acid protons are $O_2-O_7-O_9$.[12] A recent DFT calculation study, however, demonstrated that the main channel and side pocket hydroxyls are actually similar in energy and the experimentally observed low frequency band should not be simply ascribed to Brønsted acid sites located in the side pockets that have additional hydrogen-bonding interactions with the framework.[13] Instead, the authors proposed that the low-frequency shifted IR resonances were due to either protons nearby more than one Al-substituted T site, migration of H^+ due to a different site, possibly because of the two nearby Al sites, and thus a different energy landscape, or the presence of a defect within the lattice.[13]

The main motive of this present study is to determine the locations of Brønsted sites in this challenging structure by using ^{17}O and ^{1}H solid-state NMR experiments. With the development of ^{17}O isotopic enrichment methods and high magnetic field NMR instruments with high speed magic angle spinning (MAS) capabilities, high-resolution ^{17}O NMR spectra have now been collected for a variety of zeolites.[14−23] In our previous work on zeolites HY and HZSM-5, we showed that the resonances due to Si−O−Al and Si−O−Si sites in the zeolite framework, which overlap in the ^{17}O one-pulse NMR spectra, can be readily distinguished in ^{17}O multiple-quantum MAS (MQMAS) NMR spectra.[24] We also demonstrated that the ^{17}O signals from the oxygen atoms directly bound to Brønsted acid sites, which are not directly visible in the simple one-pulse experiments, can be detected and partially resolved by one-dimensional (1D) and two-dimensional (2D) $^{17}O/^{1}H$ double resonance techniques (such as $^{1}H\rightarrow^{17}O$ cross-polarization (CP), $^{17}O-^{1}H$ CP rotational echo double resonance (CP-REDOR), and $^{1}H-^{17}O$ heteronuclear correlation (HETCOR) NMR), when optimized contact times are used.[24,25] The selection of different ^{17}O signals from different hydroxyl groups, by optimizing the contact times in the cross-polarization process, is based on the fact that the CP time constants T_{IS} are governed by dipolar interactions. The dipolar coupling constant D_{IS} is defined in eq 1:

$$D_{IS} = -\left(\frac{\mu_0}{4\pi}\right)\frac{\gamma_I\gamma_S\hbar}{r_{IS}^3} \quad (1)$$

which clearly shows that the dipolar coupling has a $1/r^3$ dependence on the internuclear distance r_{IS} between the source I spins and the target S spins.[26]

In this Article, we first use ^{1}H NMR and the sorption of the basic probe molecule trimethylphosphine (TMP) to help quantify where the different proton sites are located. We then present the strategies for resolving Brønsted acid sites with different O−H bond lengths in $^{1}H/^{17}O$ double resonance NMR by varying the CP contact times. The different sites are then resolved by ^{17}O MQMAS methods, utilizing all of the different NMR approaches to extract a consistent set of NMR parameters for the different ^{1}H and ^{17}O environments. We then apply the methodology to determine the locations and nature of three types of Brønsted acid sites in zeolite H-MOR. Efforts are made to correlate the NMR parameters obtained from ^{17}O MQMAS NMR spectra with the T−O−T bond angles.

EXPERIMENTAL SECTION

Materials Preparation. Zeolite Na-Mordenite (Na-MOR) with a framework n(Si)/n(Al) ratio of 8.8 (HSZ-642NAA, $Na_{4.9}Al_{4.9}Si_{43.1}O_{96}$) was obtained from Tosoh Corp. To avoid dealumination upon heat treatment of the hydrated samples, ^{17}O enrichment was carried out on the sodium form of zeolite mordenite. Zeolite Na-MOR was first dehydrated by heating under vacuum (pressure $<10^{-3}$ Torr) from room temperature to 773 K in 4 h, and then held at this temperature for 12 h. ^{17}O isotopically enriched Na-MOR was prepared by heating dehydrated zeolite Na-MOR in $^{17}O_2$ gas (50% enriched $^{17}O_2$ from Isotec, Inc.) to 853 K and holding at this temperature for 12 h. ^{17}O-enriched zeolite NH_4-MOR was prepared by ion exchange with a 1 M NH_4NO_3 solution at ambient temperature for 12 h (repeated three times). ^{17}O-enriched H-MOR was prepared by heating ^{17}O-enriched NH_4-MOR under vacuum from room temperature to 383 K in 7 h, and then to 673 K in 12 h where the temperature was held at 673 K for a further 12 h. Non-^{17}O-enriched NH_4-MOR and H-MOR samples were prepared following the same procedures described above using nonenriched Na-MOR as a starting material instead of ^{17}O-enriched Na-MOR. The samples were stored and then packed into NMR rotors in the N_2 glovebox, prior to the NMR experiments.

TMP (99%, Alfa) and d_9-TMP (Sigma-Aldrich) were adsorbed at liquid nitrogen temperatures on the H-MOR sample prepacked in a 5 mm rotor, using glassware that is similar to the CAVERN design.[27] The loading levels were determined by the drop of pressure upon exposure of TMP to the sample, in a previously calibrated vacuum line. The samples (in the rotor) were then heated to 323 K and then held for over 4 h to equilibrate. At this point, the rotor was sealed with the rotor cap.

Solid-State NMR Spectroscopy. MAS NMR spectra were obtained with Varian Infinityplus 360, Bruker Avance 750 and 833 spectrometers, with 89 mm wide-bore 8.45, 17.6 T and 31 mm ultranarrow-bore 19.6 T superconducting magnets, respectively, in 5 mm and/or 4 mm rotors. Rotor caps with o-rings or rotor spacers with screws were used to minimize adsorption of water during the NMR measurements. ^{31}P, ^{17}O, and ^{1}H chemical shifts are referenced to 85% H_3PO_4, H_2O, and $CHCl_3$ (0.0, 0.0, and 7.26 ppm, respectively). The Hartmann−Hahn condition for the $^{1}H\rightarrow^{17}O$ CP, CP-REDOR, and 2D HETCOR NMR experiments and optimized parameters for the MQMAS experiments were determined by using the ^{17}O-enriched zeolite HY sample. Because of the very large $^{1}H-^{17}O$ dipolar coupling for O−H groups, a "mirror-symmetric" shifted-pulse CP-REDOR pulse sequence (Figure 2) was used,[28−30] rather than the standard pulse sequence often used for quadrupolar nuclei.[31,32] A standard triple-quantum MAS (3QMAS) pulse sequence with two hard pulses followed by a z-filter was used. NMR line shape simulations were performed with the Wsolids package developed by Dr. K. Eichele.[33] Simulations of the REDOR line shapes were performed by using the SIMPSON package by Nielsen and co-workers.[34] The Euler angles used in the SIMPSON simulations defining the relative orientations

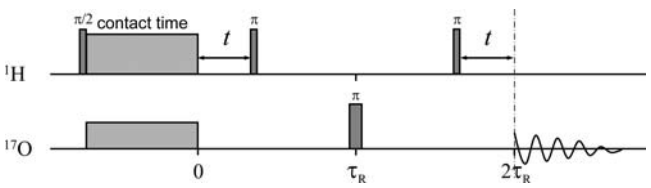

Figure 2. The NMR pulse sequence used in the $^{1}H\rightarrow^{17}O-^{1}H$ CP-REDOR experiments. "t" controls the location of the two π pulses within the rotor period, τ_R. An experiment performed without the two dephasing π pulses was used as the control experiment, providing the echo intensity after two rotor periods with essentially no dephasing under the $^{17}O-^{1}H$ dipolar coupling. Maximum dephasing occurs when $t = \tau_R/2$.

dx.doi.org/10.1021/ja301963e | J. Am. Chem. Soc. 2012, 134, 9708−9720

between the principal axis system (PAS) of the dipolar tensors with respect to the crystal fixed frame are obtained from the ab initio calculations on the model compound, zeolite HY.[25]

RESULTS AND DISCUSSION

^{1}H MAS NMR of Zeolite H-MOR. Generally speaking, ^{1}H MAS NMR spectra of bare acidic zeolites alone can rarely provide unambiguous information about different types and locations of the Brønsted acid protons. The ^{1}H MAS NMR of zeolite H-MOR, shown in Figure 3a, can be taken as a typical

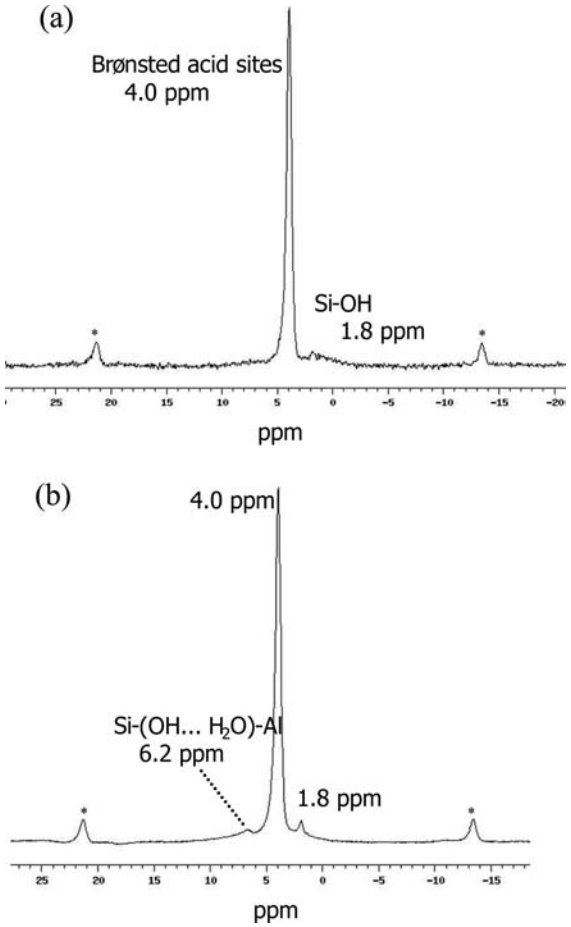

Figure 3. Single pulse ^{1}H MAS NMR spectra of (a) dry zeolite H-MOR and (b) a zeolite H-MOR sample that contains a trace amount of water, at 17.6 T, spinning speed = 13 kHz. Spinning sidebands are denoted by "*".

example of the problem. Only two major resonances at 4.0 and 1.8 ppm are resolved, which can be assigned to the Brønsted acid protons and silanol group protons, respectively. Both resonances contain shoulders to higher frequency (4.0 ppm) and lower (1.8 ppm) frequency, but at this field strength no further distinct resonances were resolved. Unfortunately, the samples when packed in nominally sealed NMR rotors can adsorb trace amounts of water upon long time exposure to atmosphere. This leads to an addition resonance at approximately 6.2 ppm, which we assign to an H_2O/Brønsted acid complex, as shown in Figure 3b.[35] Although signals due to ammonium ions occur in this chemical shift range, this assignment is ruled out because the 6.2 ppm resonance is not present in the dried sample. This sample is ^{17}O-enriched and had been stored in a rotor and studied over an extended period due to the high cost of ^{17}O enrichment.

To extract more information about the Brønsted acid protons from ^{1}H MAS NMR spectroscopy, trimethylphosphine (TMP) was employed as a basic probe molecule, because it can interact with the Brønsted acid protons to form either a neutral-hydrogen-bonded or an ion-pair complex.[36] According to the nominal chemical formula of the MOR used in this study, $H_{4.9}Al_{4.9}Si_{43.1}O_9$, there are a maximum of 4.9 Brønsted protons in each unit cell. Thus, three loading levels of 2, 3.5, and 10 TMP/u.c. were chosen, which in principle represent loading levels that are much lower, slightly lower, and much higher than the number of H^+ per unit cell, respectively, and the results are shown in Figure 4. To eliminate the strong resonance due to its methyl group protons and simplify the ^{1}H NMR spectrum, deuterated d_9-TMP was employed instead of natural abundance, unenriched TMP for the two higher loading levels (>3 TMP/u.c.). One important issue that should be considered is the maximum adsorption capacity of zeolite MOR for a large size probe molecule such as TMP, which is not necessarily the same as the number of the acidic protons. To date, no direct reports concerning the maximum adsorption capacity of zeolite MOR for TMP or any probe molecule with similar size (for instance, pyridine and benzene) are available. Furthermore, it is not straightforward to extract loading levels from most of the reported IR studies where the adsorption amount is controlled by the pressure in the IR cell. Maache et al., however, presented a quantitative IR study as a function of loading levels up to approximately 5 pyridine/u.c.,[37] while Kao et al. reported an NMR study of trimethylphosphine oxide (TMPO) loaded H-MOR with a loading level of 3 TMPO/u.c.[38] Thus, a nominal 10 TMP/u.c. represents a loading level that is not only much higher than the number of acidic sites available in zeolite HMOR, but also above the maximum adsorption amount, ensuring that the full capacity of HMOR reached. Hence, the actual loading level of this "10 TMP/u.c." sample will be lower. Most likely, the excess TMP molecules were released during the equilibration at 323 K into the large volume glass vessel of the Cavern apparatus.

^{1}H resonances are observed at 6.6−6.8 ppm and 4.0 ppm (Figure 4a and b), at loading levels of 2 and 3.5 TMP/u.c., which are assigned to TMP/Brønsted acid complexes and the remaining free Brønsted acid sites, respectively. The intense resonance at 2.1 ppm in the spectrum of the sample with 2 TMP/u.c. corresponds to methyl group protons in natural abundance TMP, which is absent when deuterated TMP is used. On increasing the loading level to 10 TMP/u.c., surprisingly the 4 ppm resonance increases in intensity, and there appear to be two poorly resolved shoulders at 5.6 and 7.0 ppm (Figure 4c). The separation between the two shoulder peaks corresponds to 500 Hz (1.4 ppm), which is similar in size to the H−P through-bond *J*-coupling seen in previous reports for similar complexes.[38] In the ^{31}P→^{1}H CP spectrum with ^{31}P decoupling (Figure 4d), a single signal at 6.4 ppm is seen on this sample. This confirms that the 7.0 and 5.6 ppm peaks are due to P−H *J*-coupling in $TMPH^+$. No peaks that can be assigned to the $TMPH^+$ doublet were seen in the spectrum of the 2 or 3.5 TMP/u.c. sample. However, when a ^{31}P→^{1}H CP MAS NMR experiment without ^{31}P decoupling was performed (Figure 4e), the doublet due to P−H *J*-coupling is now seen in the spectra of both 3.5 and 10 TMP/u.c. samples. Presumably, the CP experiment selects the rigid $TMPH^+$ ions and shows that there must be a subset of rigid $TMPH^+$ ions that give rise

dx.doi.org/10.1021/ja301963e | J. Am. Chem. Soc. 2012, 134, 9708−9720

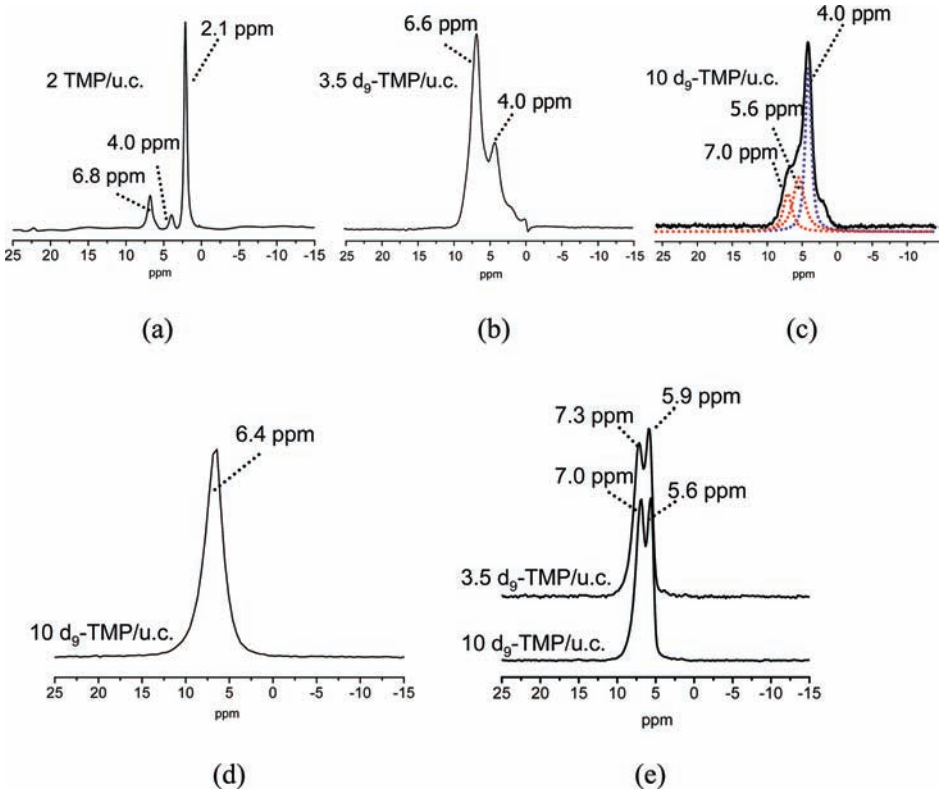

Figure 4. Single pulse ^{1}H MAS NMR spectra of the TMP/H-MOR complexes with loading levels of (a) 2 nondeuterated TMP, (b) 3.5 and (c) 10 deuterated d_9-TMP per unit cell (TMP/u.c.); (d) ^{31}P→^{1}H CP MAS NMR of 10 d_9-TMP/u.c., with ^{31}P decoupling; and (e) ^{31}P→^{1}H CP MAS NMR spectra of the two deuterated samples, without ^{31}P decoupling. Samples were equilibrated at 323 K. All spectra were acquired at a field strength of 8.45 T at room temperature.

to a doublet that is buried under the more intense 6.6 ppm resonance seen in the ^{1}H NMR spectra of the 2 and 3.5 TMP/u.c. samples in Figure 4a,b. The 6.6−6.8 ppm resonance is then assigned to more mobile TMP molecules that are H-bonded to the Brønsted acid sites, but that can hop from one binding (Brønsted acid) site to another so that no H−P dipolar interactions can be observed. It is possible that proton transfer does occur to form $TMPH^+$, but hops of these species must involve a TMP molecule, rather than a $TMPH^+$ cation, so that the *J*-coupling is lost. Thus, the overall line shape observed in the ^{1}H single-pulse experiment for the TMP species comprises resonances from two environments: (a) Brønsted protons H-bonded to mobile TMP species, and (b) rigid $TMPH^+$ cations with a covalent H−P bond formed upon complete H-transfer from the Brønsted acid oxygen to the phosphorus in TMP. At a loading level of 10 TMP/u.c., most of the Brønsted acid protons accessible to TMP molecules exist as rigid $TMPH^+$ cations giving rise to the 7.0 and 5.6 ppm doublet.

Integrals of the resonances at 6.6−6.8 (or 7.0 and 5.6 ppm) and 4.0 ppm were taken to quantify the numbers of Brønsted acid sites that interact with TMP. The sum of the two represents the total amount of acidic protons (TA), while the integral of the 4.0 ppm peak represents the residual amount of acidic protons (RA), the RA/TA ratio representing a measure of the number of inaccessible Brønsted acid sites. At 2 TMP/u.c., 20% of the total Brønsted acid protons are inaccessible to TMP. These are assigned to Brønsted acid sites located in the small cage apertures, which cannot be accessed by TMP. On increasing the loading level to 3.5 TMP/u.c, RA/TA remains constant at 25%. Surprisingly, on increasing the loading level to 10 TMP/u.c., the RA/TA ratio increases to 55%, indicating that more Brønsted acid sites are now present that are not bound to TMP, even though the TMP loading level has increased. The results suggest that 2 TMP/u.c. is already a loading level high enough to affect all accessible Brønsted acid protons. At higher loading levels of TMP, the additional molecules introduced to the cavities appear to block the access to some of the acidic protons.

In previous work, we reported a density functional (DFT) study of $TMPH^+$ ion-pair zeolite framework interactions.[39] In these studies, the $TMPH^+$ cation was shown to be stabilized by electrostatic interactions between the negatively charged framework and the protons from both methyl groups and the H−P covalent bonds. Furthermore, previous DFT calculations by others have shown that unless effective H-bonding between the protonated probe molecule and the framework O sites is possible, the Brønsted acid sites are not sufficiently acidic for H-transfer to occur.[36] Thus, the high RA/TA ratio (~55%) observed for the 10 TMP/u.c. sample is ascribed to the difficulty that the large TMP molecules have in optimizing their orientations with respect to the framework and Brønsted acid sites, due to the high population of molecules in the cages. The binding energy for TMP pointing into the side pocket must be low, due to steric constraints and again the difficulty in optimizing interactions with the zeolite framework. Thus, at higher TMP loading levels, it must become impossible for all of the $TMPH^+$ molecules to adopt ideal binding interactions with the bare Brønsted acid oxygen atoms; it is then energetically more favorable for the TMP molecules to interact with each other to form $(CH_3)_3PH$---$P(CH_3)_3$ interactions. The slight shift of 0.3 ppm to lower frequencies of the average $TMPH^+$

dx.doi.org/10.1021/ja301963e | J. Am. Chem. Soc. 2012, 134, 9708−9720

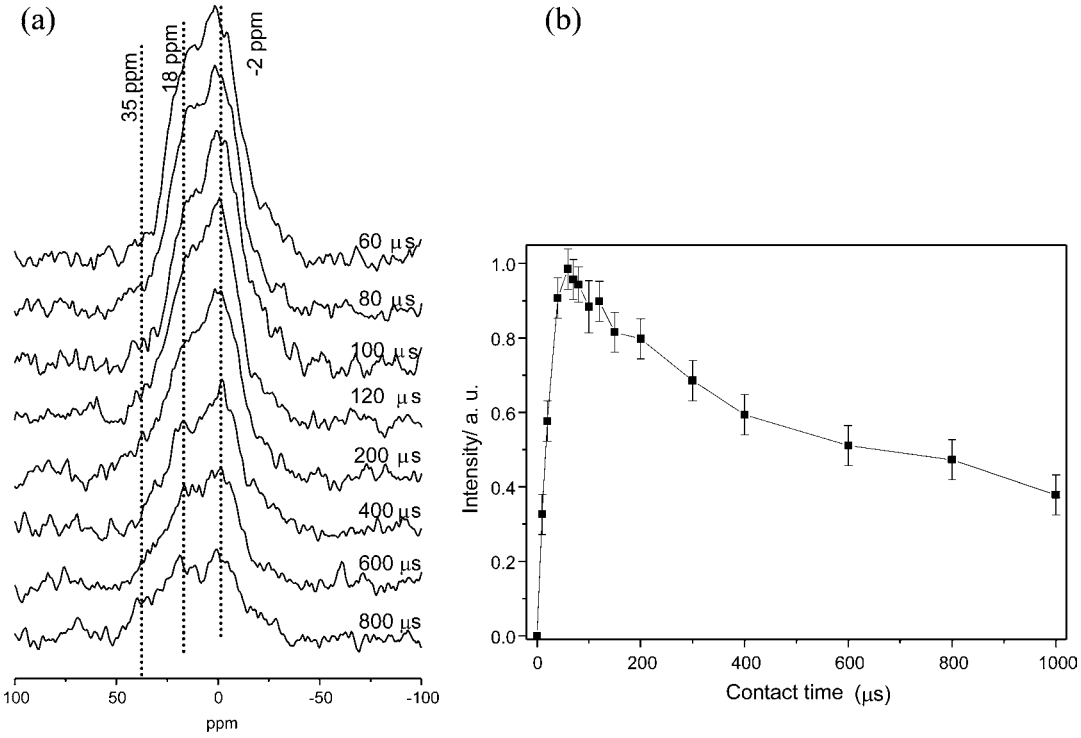

Figure 5. (a) $^{1}H \rightarrow ^{17}O$ CP MAS NMR spectra and (b) signal intensities of zeolite H-MOR acquired at 17.6 T as a function of contact time (CT), spin-lock field ~78 kHz. Error bars were added to reflect the poor signal-to-noise of some of the spectra and the error associated with the choice in the region over which to integrate the spectra.

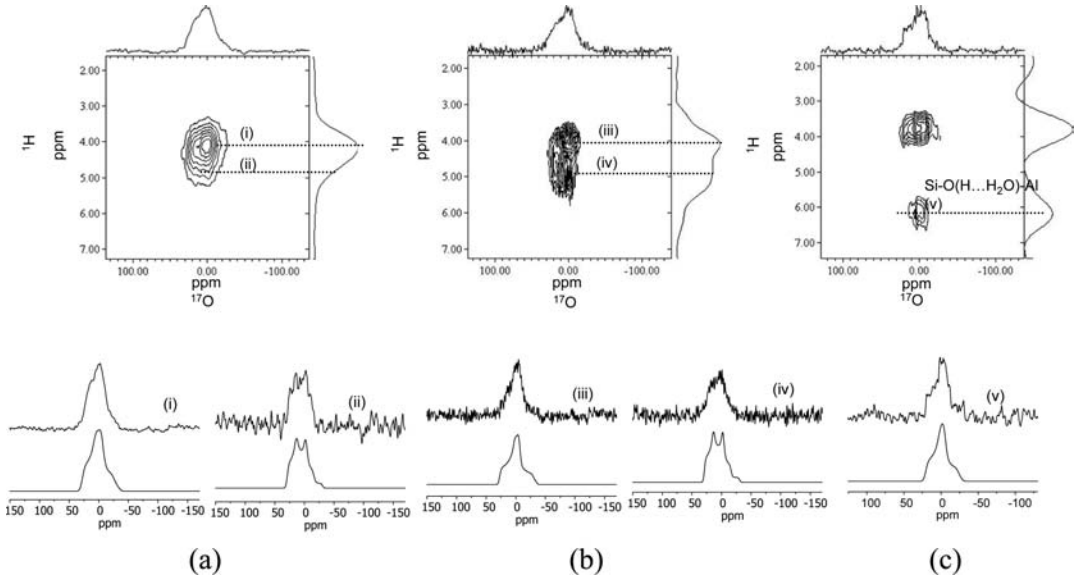

Figure 6. $^{1}H-^{17}O$ HETCOR NMR at 17.6 T of (a) dry H-MOR, contact time, 70 μs; (b) dry H-MOR, contact time, 100 μs; and (c) H-MOR containing a trace amount of H_2O, contact time, 120 μs. Recycle delay = 1 s. 64 points were acquired on the first dimension with (a,c) 7200 and (b) 4000 scans per time increment; the full 2D spectra took (a,c) 5 days + 8 h each and (b) 3 days to acquire.

shift on increasing the loading level is presumably related to the differences in H-bonding of $TMPH^+$ cations.

$^{1}H \rightarrow ^{17}O$ CP MAS NMR. CP and a series of CP-based $^{1}H \rightarrow ^{17}O$ double resonance experiments were employed to correlate the ^{1}H and ^{17}O NMR signals associated with the Brønsted acid hydroxyl groups. In our previous study on zeolite HY, the CP line shape of the ^{17}O signal from the Brønsted acid hydroxyl group could be well fit by a second-order quadrupolar line shape from a single site with a large asymmetric parameter ($\eta \approx 1$).[24] However, this is not the case for MOR, and the line shapes of the CP resonances obtained from zeolite H-MOR, shown in Figure 5a, obviously originate from more than one type of Brønsted acid site. To explore this further, the CP MAS NMR spectra were acquired as a function of contact time, CT, to attempt to separate the different resonances that contribute to the line shape on the basis of their different $^{1}H-^{17}O$ heteronuclear dipolar interactions and hence internuclear distances. The overall intensity grows rapidly reaching a

dx.doi.org/10.1021/ja301963e | J. Am. Chem. Soc. 2012, 134, 9708−9720

maximum at CT = approximately 60 μs, dropping steadily thereafter (Figure 5b). The behavior is similar to our previous results for zeolite HY and HZSM-5, where maximum signal intensities were seen at CT = 60 and 80 μs, respectively, the slightly shorter CT value for MOR suggesting that the apparent (average) O−H bond length in MOR is similar to that in HY but shorter than that in HZSM-5.[24] However, the mobility of the protons also needs to be considered, and for HZSM-5 this was significant. Thus, a shorter contact time can also be an indication of less motion. (Note that we have not performed any detailed analyses of the effect of the $T_{1\rho}{}^{H}$ and $T_{1\rho}{}^{O}$'s (the relaxation times of ^{1}H and ^{17}O, respectively, in the rotating frame) on these CP curves. If these values are short, they will also affect the position of apparent CP maxima, and an accurate analysis of O−H distances would require that we took these values into account.) More importantly, the line shape varies noticeable with CT. At the shortest contact time shown in Figure 5a, 60 μs, the line shape is characterized by two discontinuities at −2 and 18 ppm. The line shape is similar from 60 to 80 μs. However, as the contact time increases further, the line shape changes noticeably, with components at higher frequency (around 35 ppm) starting to grow in relative intensity.

2D ^{1}H−^{17}O HETCOR NMR. Because one-dimensional CP MAS NMR spectroscopy cannot resolve the resonances from all of the different Brønsted acid sites, 2D ^{1}H−^{17}O HETCOR NMR spectroscopy has been employed to attempt to separate the ^{17}O signals from each distinct site on the basis of different and characteristic O−H bond lengths/H-bonding and hence specific ^{1}H chemical shift values. Two sets of contact times were chosen in this and the subsequent ^{17}O−^{1}H double resonance experiments: longer contact times (100−120 μs) and shorter contact times (60−80 μs) close to the CP build-up curve maximum. When a short contact time of 70 μs was applied (Figure 6a), only one resonance centered at ∼4.0 ppm can be observed in the ^{1}H dimension. The simulation result (including quadrupolar and chemical shift parameters) of the slice taken at this position (slice (i), δ_{CS} ^{1}H = 4.0 ppm) is shown in Table 1, and the line shape can be well described by a single set of quadrupolar parameters (with a value of η of 0.7), unlike the projection of sum on the ^{17}O dimension. A slice taken at (ii) (δ_{CS} ^{1}H = 4.8 ppm) suggests that a second component may be buried under the 4.0 ppm ^{1}H resonance, with an associated ^{17}O resonance with a smaller value of η of approximately 0.45. This second component is clearly revealed in Figure 6b, which shows the ^{17}O−^{1}H HETCOR spectrum of H-MOR obtained with longer contact time of 100 μs, and the slices taken at positions (iii) and (iv) show oxygen environments that are similar to those that were resolved in slices (i) and (ii) in Figure 6a. The poorer signal-to-noise of slices (ii) and (iv) is directly related to the low intensity of the corresponding resonance in the ^{1}H dimension. The greater intensity of the broad ∼4.8 ppm resonance in the 100 μs contact time spectrum suggests that the ∼4.8 ppm resonance is associated with a longer O−H bond length. The spectrum confirms that there is more than one acidic hydroxyl group in zeolite H-MOR.

Table 1. NMR Parameters of ^{17}O Atoms Directly Bound to Brønsted Acid Sites Obtained from Simulations of the HETCOR NMR Slices

slice	δ_{CS} (^{1}H) (ppm)	QCC (MHz) (±0.05)	η (±0.1)	δ_{iso} (ppm) (±1)
(i)	4.0	6.3	0.7	28
(ii)	4.8	6.4	0.45	31
(iii)	4.0	6.2	0.8	27
(iv)	4.8	6.4	0.45	31
(v)	6.2	5.5	0.8	21

Figure 6c shows the ^{17}O−^{1}H HETCOR spectrum of the sample that has absorbed a trace amount of water, having been left in an NMR rotor (albeit in a glovebox) for extended periods of time. A contact time of 120 μs was adopted to select longer O−H bonds, possibly elongated by H-bonding to water. A new resonance at 6.2 ppm is now seen in the ^{1}H dimension, which we assign to an acidic proton H-bonded to a trace amount of H_2O, consistent with the single pulse ^{1}H MAS NMR spectrum of the same sample (Figure 3). The absence of a resonance at 4.8 ppm on the ^{1}H dimension suggests that any water that is present is H-bonded to the zeolite framework. More importantly, the resonance due the Brønsted acid site seen in the dry samples is no longer present, indicating that water may be bound to these sites; simulation of the slice taken at δ_{CS} ^{1}H = 6.2 ppm indicates that the local environment around the relevant oxygen atoms has dramatically changed upon adsorption of water, with the quadruple coupling constant (QCC) decreasing to approximately 5.5 MHz, and the ^{17}O isotropic chemical shift decreasing to 21 ppm.

^{1}H→^{17}O−^{1}H CP-REDOR Spectroscopy. REDOR experiments were then performed to extract the O−H distances for the different Brønsted acid sites in MOR. The experimental CP-REDOR line shapes, as a function of the time before the first dephasing pulse (t) (see Figure 2), at contact times of 80 and 120 μs are shown in Figure 7a and b, respectively, where these contact times were chosen so as to obtain line shapes with different relative contributions from the different components present in MOR. As discussed in our previous study on zeolite HY, the REDOR dephasing behavior is not uniform across the whole second-order quadrupolar line shape,[24] two dotted lines having been added to these figures to illustrate this more clearly. REDOR fractions were then extracted by integrating the isotropic resonances only (Figure 8). (The sidebands were not included due to signal-to-noise concerns.) The REDOR fractions increase reaching a maximum, when "t" is approximately 20 and 25 μs, for the data with contact times of 80 and 120 μs, respectively. The slower dephasing and lower REDOR fraction when a contact time of 120 μs is used indicates that some O−H groups with either longer O−H distance and/or more mobile protons have been selected.

The two different quadrupolar line shapes (and associated NMR parameters) identified in the HETCOR experiments were then adopted to help analyze the REDOR data. A simulation of these two line shapes, which we refer to as the "large" and "small η" sites (Figure 9a and b), shows that they give rise to discontinuities that are consistent with the experimental spectra, the discontinuity at −2 ppm resulting from the overlap of the most intense discontinuity of the large η resonance and the most intense lower frequency discontinuity of the small η resonance, while the discontinuity at 18 ppm largely results from the higher frequency discontinuity of the small η resonance. To illustrate this, a two-site simulation with "large" and "small η" sites at a 1:1 ratio is shown in Figure 9c. This simulated line shape mimics the experimental result (Figure 9d) well, indicating that the overall line shape can be considered as a sum of these two types of line shapes. The ^{17}O

dx.doi.org/10.1021/ja301963e | J. Am. Chem. Soc. 2012, 134, 9708−9720

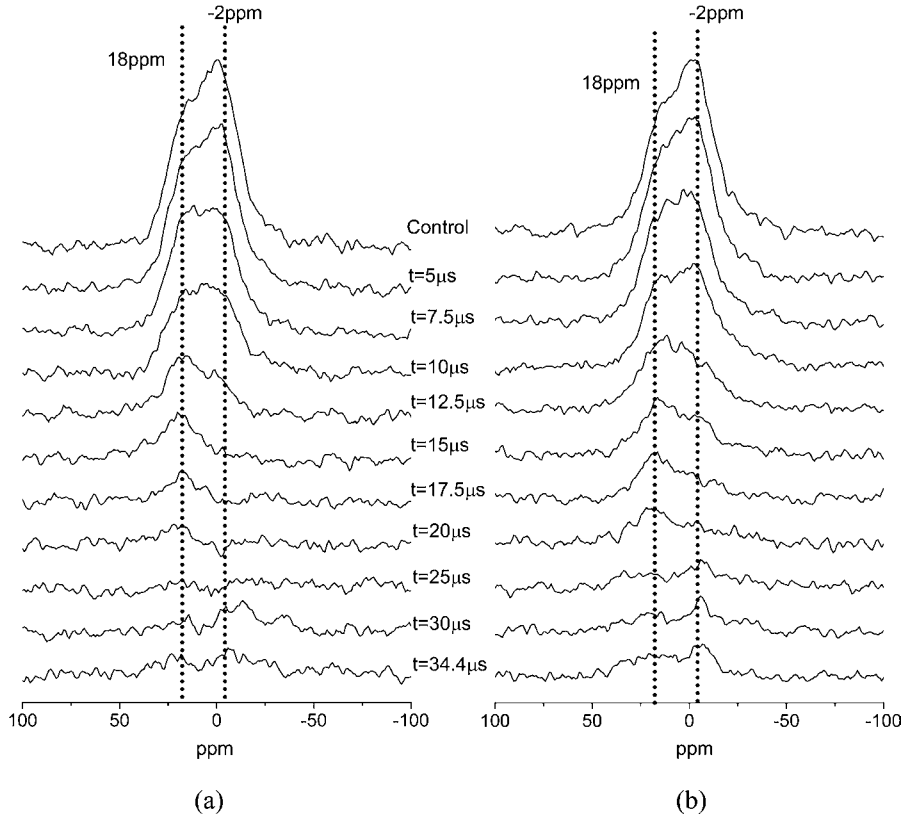

Figure 7. The plot of $^{1}H \rightarrow {}^{17}O-{}^{1}H$ CP-REDOR NMR spectra as a function of the shift of the first dephasing pulse (at time t) with contact times of (a) 80 and (b) 120 μs, at 17.6 T. Spinning speed, 13 kHz; recycle delay, 1 s.

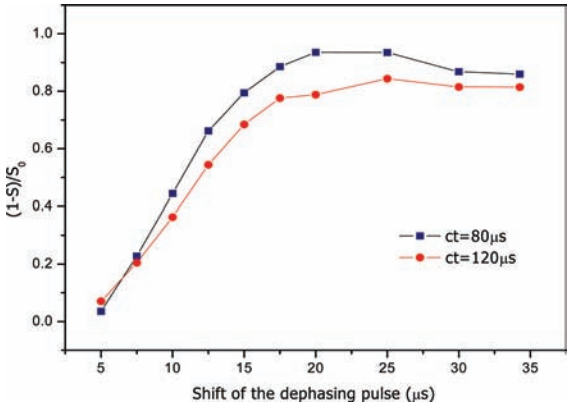

Figure 8. $^{1}H \rightarrow {}^{17}O-{}^{1}H$ CP-REDOR fraction $(1 - S/S_0)$ measured as a function of the shift of the first dephasing pulse (at time t), extracted from the data shown in Figure 7.

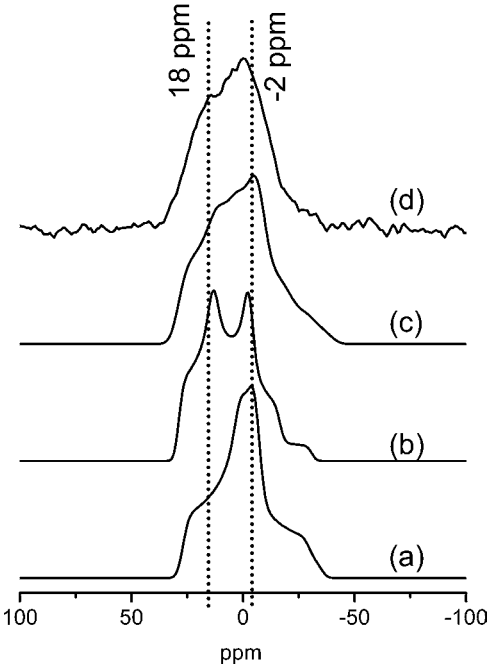

Figure 9. Scheme for the line shape analysis. Simulations of the (a) large η and (b) small η sites resolved from the 2D $^{17}O-{}^{1}H$ HETCOR spectra. (c) Simulation with two sites with large η and small η 1:1 ratio. (d) The experimental spectrum of the control experiment obtained with the contact time of 80 μs.

resonance with the large η value is from oxygen atoms more tightly bound to the protons and can be enhanced by using shorter contact times. In contrast, the resonance with a small η value corresponds to an oxygen environment with a longer O–H distance/stronger motion and can be selectively enhanced by using a longer contact time.[40] Numerical simulations of the large η site (NMR parameters extracted from the $^{17}O-{}^{1}H$ HETCOR spectra) with several chosen dipolar coupling constants are shown in Figure 10a–c, while those for the small η site are shown in Figure 10d–f. The slight mismatch of the chemical shift between the experimental data and simulations is ascribed to the presence of more than one Brønsted acid oxygen site in zeolite HMOR while the simulation was performed by using a single-site model. The simulations provide a framework with which to examine the experimental dephasing behaviors. For the shorter contact time

dx.doi.org/10.1021/ja301963e | J. Am. Chem. Soc. 2012, 134, 9708–9720

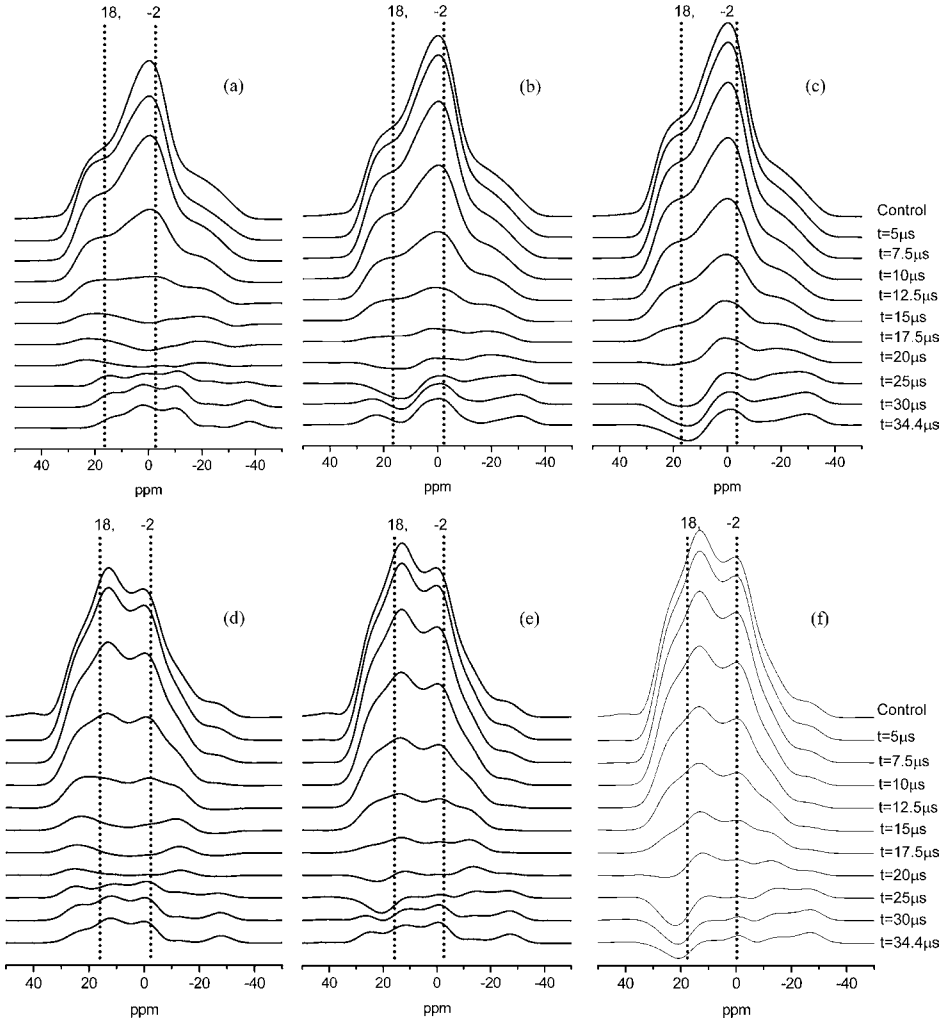

Figure 10. NMR line shape simulations performed with the SIMPSON package.[34] (a–c) Simulations performed with dipolar coupling constants of 22 346, 17 850, and 15 000 Hz, respectively. The NMR parameters used in the simulations are δ_{CS} = 27.5, QCC = 6.25 MHz, and η = 0.75 (the average of the values taken from the simulation results of the "large η" sites resolved in the $^{17}O-^{1}H$ HETCOR spectra). (d–f) Simulations performed with the same three dipolar coupling constants but with different NMR parameters (δ_{CS} = 31, QCC = 6.4 MHz, and η = 0.45) corresponding to the values of the "small η" sites resolved in the $^{17}O-^{1}H$ HETCOR spectra.

of 80 μs, the experimental intensity near the discontinuity at −2 ppm decreases rapidly, reaching a minimum at t = 20 μs and then increasing in intensity. In contrast, the discontinuity at 18 ppm dephases more slowly, reaching a null point at t = 25–30 μs. On the basis that the −2 ppm discontinuity is more strongly affected by the large η site, this appears to suggest that the dipolar coupling constant is in the range of 22–18 kHz (O–H distance 0.90–0.97 Å). The 120 μs contact time spectra should, according to our model, contain a larger contribution from the small η site. The difference in the behavior of the two sets of spectra is not dramatic, the dephasing of the intensity around −2 ppm being slightly slower for the 120 μs spectra (see, for example, the spectrum at t = 15 μs), never becoming negative. Although by no means definitive, the results suggest an increasing (small) contribution from a component with a longer apparent O–H distance (0.97–1.03 Å).

^{17}O MQMAS. ^{17}O MQMAS NMR spectroscopy was then performed so as to observe both protonated and non-protonated sites in one experiment and compare the parameters with those obtained above. Our assignments of the different sites and the choice of optimum MQMAS parameters were aided by our previous ^{17}O MQMAS NMR study on zeolite HY.[41] The two-dimensional (2D) ^{17}O MQMAS NMR spectrum of zeolite H-MOR and its F_1/F_2 projection acquired at a magnetic strength of 19.6 T are shown in Figure 11. The isotropic (F_1) projection shows five resonances with centers of gravity δ_1 of 19, 24, 28, 41, and 45 ppm, which can be assigned to framework oxygen sites in Si–O–Al (19, 24, and 28 ppm, green circle) and Si–O–Si (41 and 45 ppm, blue circle) linkages, respectively. The NMR parameters for the Si–O–Si and Si–O–Al linkages were extracted by simulating the slices of the F_2 dimension, and the NMR parameters are listed in Table 2. The shifts δ_1 and δ_2 can be used to extract the values for isotropic chemical shift, δ_{CS}, and quadrupolar product, P_Q, directly, without simulating the F_2 dimension. For a spin I = 5/2 nucleus, these parameters are given by:

$$\delta_{iso} = \frac{17}{27}\delta_1 + \frac{10}{27}\delta_2 \quad (2)$$

$$P_Q = \frac{\nu_0}{25}\sqrt{\frac{85(\delta_1 - \delta_2)}{1296}} \quad (3)$$

dx.doi.org/10.1021/ja301963e | J. Am. Chem. Soc. 2012, 134, 9708–9720

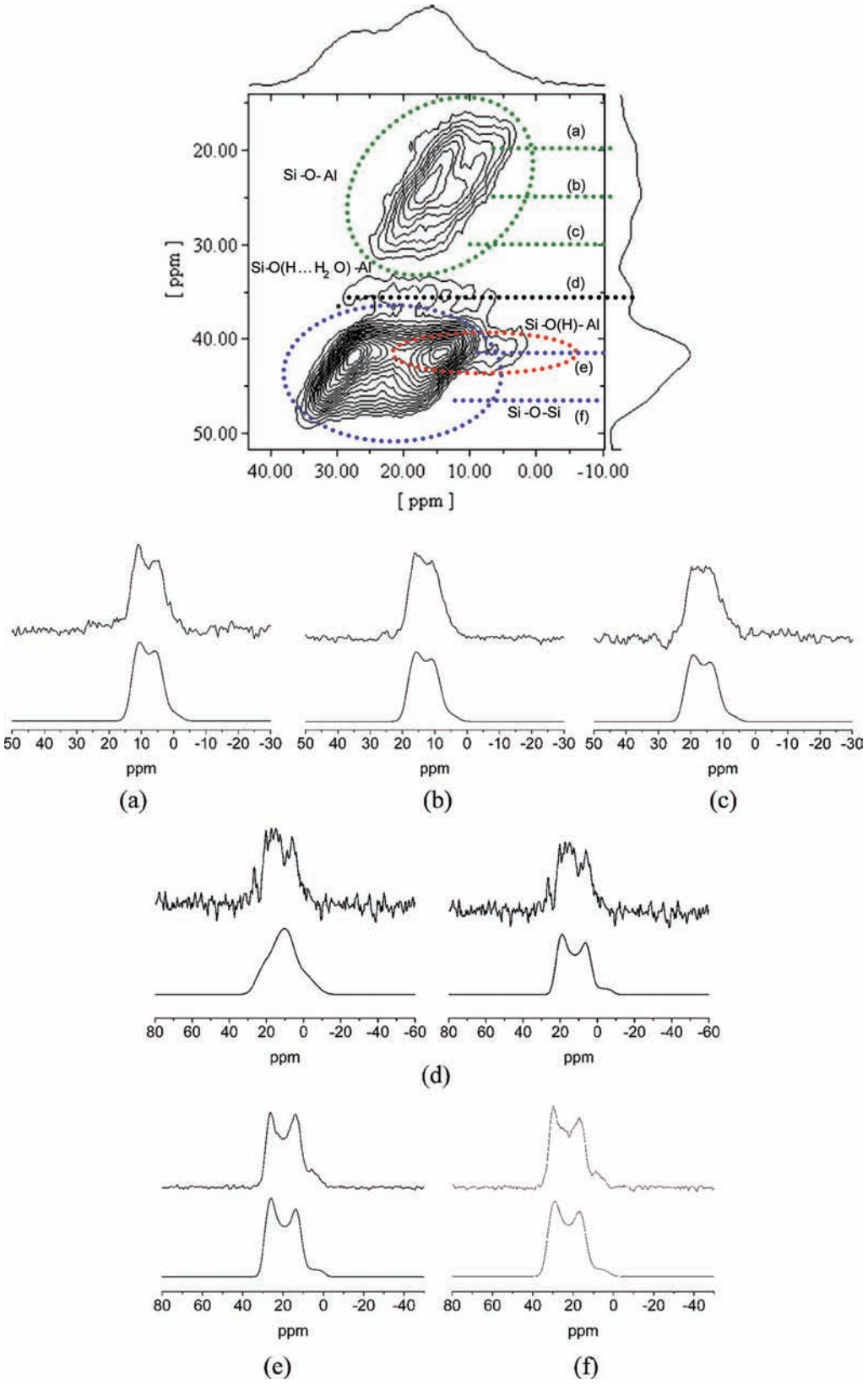

Figure 11. 2D-^{17}O MQMAS NMR spectrum of ^{17}O-enriched H-MOR acquired at 19.6 T, with a spinning speed of 10 kHz and recycle delay of 0.5 s. 32 points were acquired on the first dimension with 12 600 scans per time increment; the full 2D spectrum took 2 days + 8 h to acquire. The projections (sum) of the F_2 and F_1 dimensions are shown on the above and right sides of the 2D-spectrum, respectively. The slices of anisotropic dimension at (a) 19, (b) 24, (c) 28, (d) 35, (e) 41, and (f) 45 ppm in the isotropic dimension (top), are compared to simulations performed with the WSolids NMR package (bottom), plotted below. The simulation parameters are shown in Table 2. The dotted lines in 2D spectra show where the slices are taken. Note: In (d) due to poor S/N, the spectrum is simulated with both η = 0.7 (left) and η = 0.2 (right).

dx.doi.org/10.1021/ja301963e | J. Am. Chem. Soc. 2012, 134, 9708−9720

Table 2. NMR Parameters of Framework Si−O−Si and Si−O−Al Linkages in Zeolite H-MOR from Experimental MQMAS Data and Simulations[a]

				values calculated from δ_1 and δ_2		simulation data			
site	slice	δ_1 (ppm)	δ_2 (ppm)	δ_{iso} (ppm)	P_Q	QCC (MHz)	η	δ_{iso} (ppm)	P_Q
Si−O−Al	(a)	19	8	15	3.7	3.8	0.2	15	3.8
	(b)	24	13	20	3.8	3.8	0.25	20	3.8
	(c)	28	16	24	4.0	4.0	0.25	24	4.0
hydrated site	(d)	35	14	26	5.2	5.3	0.7	26	5.7
						5.1	0.2	23	5.1
Si−O−Si	(e)	41	19	33	5.4	5.4	0.2	33	5.4
	(f)	45	23	36	5.4	5.4	0.2	36	5.4

[a] δ_2's and δ_1's are the observed center of gravities of the resonances in the anisotropic (F_2) and isotropic (F_1) dimensions for oxygen atoms at 19.6 T in zeolite H-MOR, respectively. Values of P_Q and δ_{iso} were calculated from the observed shifts of center of gravity of the resonances, using eqs 2 and 3. Values of QCC, η, and δ_{iso} were obtained from the Wsolid simulation result of each slice. The differences between the values of P_Q calculated with eq 4 using the NMR parameters obtained by simulation data and the predicted values of P_Q extracted from the observed center of gravities can be taken as a measure of the reliability of the simulations.

$$P_Q = \mathrm{QCC}\sqrt{1 + \frac{\eta^2}{3}} \quad (4)$$

where ν_0, QCC, and η are the Larmor frequency, the quadrupolar coupling constant, and the asymmetry parameter, respectively. The predicted δ_{iso} and P_Q have been used to examine the results of line shape simulation. Conversely, the values of δ_1 and δ_2 can be predicted, if δ_{iso} and P_Q are known.

A signal is observed at δ_1= 35 ppm (slice (d)), which has quite distinct values for δ_{iso} and P_Q, as determined from δ_1 and δ_2, from those of the Si−O−Si and Si−O−Al sites. We tentatively assign this site to the Brønsted acid site contaminated with a trace amount of water that was resolved in the $^{17}O-^{1}H$ HETCOR experiment, but note that the asymmetry parameter of this site appears quite different from that obtained earlier. The source of this error is not clear, but is likely related to the poor S/N ratio of these spectra and the difficulty in exciting all parts of the powder uniformly.

Previous MQMAS and double rotation (DOR) NMR results[18,21] for zeolites with high Al contents indicate that there is a linear correlation with a negative linear coefficient between the ^{17}O isotropic chemical shift and the Si−O−Al bond angle (δ/ppm = -0.65α/deg + 134)[17] or (δ/ppm = -0.71α/deg + 143.7).[18,21] On the basis of these correlations, the MOR Si−O−Al resonances at δ_1 = 14.6, 20, and 23.6 ppm correspond to Si−O−Al bond angles of 182−184°, 174−175°, and 169−170°, respectively. In contrast, according to crystallographic studies on zeolite H-MOR[4] and its deuterated form D-MOR,[5] while the T−O−T bond angles are distributed over a wide range of 139−180°, only the O_4, O_6, and O_8 T−O−T bond angles are larger than 165°. Two possible explanations for this discrepancy can be proposed. First, the MOR bond angles determined by crystallography will be dominated by Si−O−Si angles, and the Si−O−Al angles may be quite different. Second, the correlation between Si−O−Al bond angles and the ^{17}O isotropic chemical shifts may vary from sample to sample because they will also depend on the nature of the charge balancing cation/proton and its proximity to the oxygen atom.[19]

The distribution of T−O−T bond angles in zeolites H (D)-MOR, HY, and HZSM-5 is given in Table 3. The T−O−T angles in zeolite HY are distributed over a much narrower range with smaller values of 135.7−144.6° in contrast to those of zeolite H (D)-MOR, while those of HZSM5 have intermediate

Table 3. Structural Parameters for the Brønsted Acid Sites of Zeolites D(H)-MOR, H-Y, and H-ZSM-5 As Reported in the Literature

zeolite	site	T−O distance (Å)	T−O−T angle (deg)	O−D(H) distance (Å)
D-MOR[5]	O_1	1.55(T_1-O_1)	146	
		1.60(T_3-O_1)		
	O_2	1.58(T_2-O_2)	146	
		1.63(T_4-O_2)		
	O_3	1.60(T_1-O_3)	147	
		1.63(T_2-O_3)		
	O_4	1.61(T_3-O_4)	168	
		1.60(T_4-O_4)		
	O_5	1.65(T_2-O_5)	139	1.01
	O_6	1.63(T_1-O_6)	165	1.01
	O_7	1.61(T_1-O_7)	139	
	O_8	1.59(T_2-O_8)	180	
	O_9	1.63(T_3-O_9)	160	1.00
	O_{10}	1.62(T_4-O_{10})	152	1.00
H-Y[42]	O_1	1.677	135.7	0.83
	O_2	1.632	144.6	1.02
	O_3	1.654	139.8	0.98
H-ZSM-5[43]	O	1.57−1.60	153−169	

values. On the basis of data extracted from our previous ^{17}O MQMAS study of zeolite HY,[41] the measured ^{17}O isotropic shifts for the Si−O−Al groups, δ_{iso} = 27.5−33.3 ppm, give predicted angles of 149.5−157.5°, using the correlations given above. Again, the predicted angles are larger than those obtained by diffraction (Table 3). Again, this suggests that while a linear correlation δ/ppm = $k\alpha$/deg + β may hold, the specific values of the coefficients k and β may vary for different zeolites. We hope that future first principles calculations of NMR chemical shifts may help in the assignment of these resonances and in providing improved correlations.

The Nature of the Brønsted Acid Site at $\delta_{CS}{}^{1}H$ = 4.8 ppm. In the TMP adsorption experiments performed with different loading levels, the ^{1}H resonance of the residual acid sites inaccessible to TMP probe molecules is centered at ~4.0 ppm. This suggests that the acid site that corresponds to the ^{1}H resonance at ~4.8 ppm is located in the 12-ring main channel and hence can be easily accessed by TMP probe molecules. The $^{1}H-^{17}O$ HETCOR experiment of the sample containing a trace

dx.doi.org/10.1021/ja301963e | J. Am. Chem. Soc. 2012, 134, 9708−9720

Table 4. Possible Locations of Brønsted Acid Sites on the Basis of NMR Results

accessibility to TMP	^{1}H NMR shift (ppm)	amount	location	possible sites	ruled out by structural restrictions[a]
inaccessible	4.0	20−25% (~1/u.c.)	8-ring channel or intersection of 8-ring channel and side pocket	O_1, O_6, O_9	O_6
partially accessible	4.0	25−30% (~1/u.c.)	intersection of 12-ring channel and side pocket	O_5	
fully accessible	4.8	~1/u.c. 45−50% (~2/u.c.)	12-ring	O_2−H−O_2	
	4.0	~1/u.c.		O_2, O_3, O_7, O_{10}	O_3, O_7

[a]The following two restrictions are applied: (1) in each unit cell, only one T_1/T_2 site can be occupied by Al; and (2) only one Brønsted site can be accommodated in the same tetrahedron.

amount of water further confirms that this δ_{CS}^{1}H = 4.8 ppm resonance is associated with Brønsted acid sites that were the most easily attacked by the adsorbed water molecules. The ^{17}O signal of the oxygen site connected with this proton site can be favored by a slightly longer contact time in experiments involving cross-polarization excitation. This is ascribed to a longer O−H distance and/or a more mobile proton. Given the fact that tightly bound bridging O−H group and bare Si−O−Al give rise to η values ~1 and ~0, respectively, the smaller asymmetric parameter η extracted from HETCOR experiment as compared to the other acidic site oxygen also suggests that the proton at this Brønsted acid site is loosely bound to the oxygen atom. On the basis of the above observations, these results are best explained if this proton is due to an acidic hydroxyl group H-bonded to nearby framework oxygen.

The typical oxygen-to-oxygen distance required for moderate to weak H-bonding varies in the range of 2.4−2.7 Å.[44,45] A close check of the framework structure identifies the following pairs: O_2−O_5 2.522 Å, O_6−O_1 2.643 Å, O_1−O_9 2.607 Å, and O_2−O_2 2.677 Å. Among the four choices above, the oxygen pairs of O_2−O_5 and O_2−O_2 fulfill the requirement that both oxygen atoms are located in the 12-ring main channel. The configuration of the O_2−O_2 pair appears the most likely because the sp^3 orbitals of both oxygen atoms point into the center of the 12-ring channel. As shown by Kobe et al. in their ^{2}H NMR study of Brønsted acid sites in zeolite D-MOR,[46] the bridging OD groups undergo 2-site exchange involving a change in orientation of the OD bond of 109°. Although these authors suggested that the hops involved reorientation of the OD bonds on the same oxygen atom, the reorientation angle (109°) is also consistent with a hop between two O_2 atoms. A hop between two O_2 sites, however, would suggest that both O_2 sites are adjacent to an Al-substituted T site, either because one T4 site or two nearby T2 were substituted. Double substitution is consistent with the suggestions that emerge from the DFT study of Dominguez-Soria.[13] Furthermore, this hopping is consistent with the relatively long apparent O−H distance and reduced REDOR fraction observed for MOR as probed the ^{17}O−^{1}H dipolar coupling.

The Locations of Brønsted Acid Sites in Zeolite H-MOR. *Assumptions.* As discussed above, the zeolite H-MOR used in this study possesses a Si/Al ratio of 8.8 with an ideal composition of $H_{4.9}Al_{4.9}Si_{43.1}O_{96}$. However, as reported by many groups and on the basis of ammonia sorption, conductometric titration, and temperature-programmed desorption (TPD) experiments, the actual concentration of Brønsted protons can be lower (up to 20%) than the concentration calculated from the Si/Al ratio, presumably due to dealumination.[47−51] Thus, to perform the subsequent analysis, we assume that the total number of Brønsted protons in one unit cell is about 4, a number that is also consistent with the TMP sorption experiments. To determine the locations of Brønsted acid sites requires that we allocate these 4 H atoms over the 96 O atoms (10 inequivalent O sites) in one unit cell.

In IR studies of zeolite H-MOR with probe molecules, all of the IR stretches are affected by small probe molecules such as ammonia.[50] On the basis of this fact, Alberti deduced that, among these 10 inequivalent O sites, O_4 and O_8 pointing toward the chains of 5-rings cannot be active as Brønsted acid sites,[12] because they are inaccessible to molecules as small as ammonia. Hence, in the following discussion, we will only consider the other 8 framework oxygen sites as possible Brønsted acid sites.

The locations of acidic protons are directly related to the locations of Al in the framework. The two crystallographic refinements[4,52] and ab initio calculations[53] have all suggested that two sites, T_3 and T_4, in 4-rings are preferentially occupied by Al. A ratio for the occupancy of the sites of $(T_3+T_4)/(T_1+T_2)$ = 3:1 has been estimated by Alberti.[12] This analysis suggests that among the 4−5 Al atoms in a single unit cell, only about 1 Al sits on either a T_1 or T_2 site.

Information Extracted from NMR Results. The Brønsted protons in zeolite H-MOR can be divided into four categories (Table 4), on the basis of NMR results.

Category I (Inaccessible to TMP Molecules). According to the TMP adsorption experiments, about 20−25% of all of the Brønsted acid sites in zeolite H-MOR (~1/u.c.) are not accessible to TMP molecules at all loading levels. The side pocket 8-ring window connecting the 12-ring and the 8-ring channels is about 3.4 × 4.8 Å in diameter (Figure 12a), while the estimated diameter of a TMP molecule obtained by measuring the distance between two distant hydrogen atoms in the −CH_3 groups is 5.5 Å (Figure 12b). Thus, the TMP

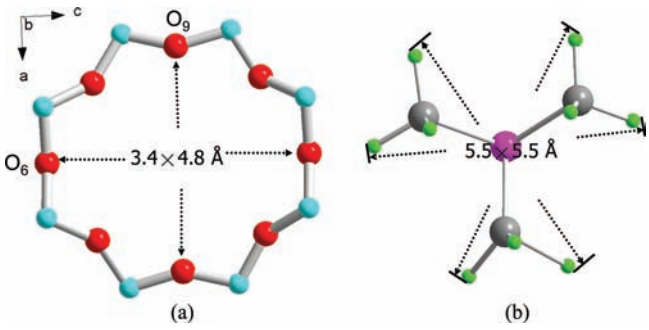

Figure 12. Measurements of (a) side pocket 8-ring of zeolite H-MOR and (b) the TMP molecule.

dx.doi.org/10.1021/ja301963e | J. Am. Chem. Soc. 2012, 134, 9708−9720

molecules cannot reach the 8-ring channel through the side pocket due to the steric hindrance arising from the three methyl groups. Hence, the acidic sites that are not accessible to TMP probe molecules must be located either on O_1 and on O_9 pointing into the center of the 8-ring channel, or at O_6 at the intersection of 8-ring and the side pocket.

Category II (Partially Accessible to TMP Molecules). The ^{1}H MAS NMR spectrum of a H-MOR sample nominally loaded with 10 d_9-TMP/u.c. shows a high RA/TA ratio (~55%). This suggests that the large populations of $TMPH^+$ cations and TMP molecules in the main channel at this loading level can block the access to about 20% acidic sites (~1/u.c.), which were originally accessible to TMP at lower loading levels. This population should correspond to acidic sites located at the intersection of the 12-ring and the side pocket. The oxygen atoms on this 8-ring at the intersection are O_2 and O_5. The acidic hydroxyl group, which is located on O_2, points into the center of the 12-ring channel and is fully accessible to TMP probe molecules. Hence, O_2 does not belong to this category. However, whether the acidic proton located on O_5 points into the main channel or the side pocket is still not clear.[5,12] The results presented here suggest that the O_5–H bond points toward the side pocket and O_5 is a reasonable location for a Brønsted acid site.

Categories III and IV (Fully Accessible to TMP Molecules). According to the TMP loading result with the loading level of 10 d_9-TMP/u.c., about 45–50% of the Brønsted acid sites in zeolite H-MOR are located in the 12-ring main channel (~2/u.c.). A subset of these Brønsted acid sites corresponds to the environment that gave rise to resonance at 4.8 ppm. This resonance has already been ascribed to the H-bonded O_2–O_2 pair. Given the fact that there is only one 12-ring in each unit cell, this pair corresponds to a Brønsted proton shared between two unit cells.

There should be one additional Brønsted acid site/u.c. in the main channel with a similar chemical shift (4.0 ppm) as the protons located in 8-ring and side pocket. To identify the possible locations of these sites, a more careful investigation of the structure is necessary. Because O_5, which is bound to the T_2 site via the linkage T_2–O_5–T_2, has been determined to be a potential location of one of the acidic sites, this suggests at least a partial occupancy of the T_2 site with Al. Because, on the basis of the analysis of Alberti et al., the occupancy of the T_2 and T_1 sites is low with only 1 Al atom sitting on a T_1/T_2 site per unit cell, it appears that oxygen sites nearby T_1 are less likely (but cannot be definitively ruled out). The sites involving T_1 are O_6 (T_1–O_6–T_1), O_7 (T_1–O_7–T_1), and O_3 (T_1–O_3–T_2). The remaining possible Brønsted proton sites inside the 12-ring channel are O_{10} (T_4–O_{10}–T_4) and O_2. Of these possibilities, the latter two appear the most plausible, simply based on the suggested occupancies of the T sites.

CONCLUSIONS

A series of ^{17}O–^{1}H cross-polarization double resonance experiments (CPMAS, CP-REDOR, and HETCOR NMR) were used to identify different Brønsted acid sites in zeolite H-MOR. The relative contribution to the ^{17}O spectrum from different Brønsted acid sites associated with different O–H distances was modified by varying the contact time in the CP experiment. This approach was used to distinguish between two types of acidic hydroxyl groups with longer and shorter O–H distances. The experimental results suggest that the site with the longer O–H distance corresponds to two adjacent O_2 atoms on the wall of 12-ring main channel sharing one proton through H-bonding. ^{1}H MAS NMR spectroscopy in combination with loading studies involving the basic probe molecule trimethylphosphine showed that about 20–25% acidic hydroxyl groups are located in 8-ring channels, 25–30% are located at the intersections of the side pockets and main channels, and the rest (45–50%) are located in the 12-ring main channels.

By carefully examining the structure, it has been concluded that there are four most plausible locations for Brønsted acid sites in zeolite H-MOR: (a) O_1/O_9, pointing into the center of the 8-ring channel and inaccessible to TMP probe molecules; (b) an adjacent pair of O_2 atoms sharing one proton through H-bonding; (c) O_5, which points slightly toward the side pocket; and (d) O_{10}, pointing into the center of the 12-ring. It is hoped that similar approaches and methodologies can be used to examine proton distributions in other zeolites and catalytic systems.

AUTHOR INFORMATION

Corresponding Author

cpg27@cam.ac.uk

Notes

The authors declare no competing financial interest.

ACKNOWLEDGMENTS

We thank Dr. Boris Itin for his help in obtaining the 17.6 T NMR data. Financial support was provided by the DOE via grant DEFG0296ER14681.

REFERENCES

(1) Bowers, C. R.; Storhaug, V.; Webster, C. E.; Bharatam, J.; Cottone, A.; Gianna, R.; Betsey, K.; Gaffney, B. J. *J. Am. Chem. Soc.* **1999**, *121*, 9370.
(2) Corma, A. *Chem. Rev.* **1995**, *95*, 559.
(3) Derouane, E. G.; Andre, J. M.; Lucas, A. A. *J. Catal.* **1988**, *110*, 58.
(4) Mortier, W. J.; Pluth, J. J.; Smith, J. V. *Mater. Res. Bull.* **1975**, *10*, 1319.
(5) Martucci, A.; Cruciani, G.; Alberti, A.; Ritter, C.; Ciambelli, P.; Rapacciuolo, M. *Microporous Mesoporous Mater.* **2000**, *35–6*, 405.
(6) Jacobs, P. A.; Mortier, W. J. *Zeolites* **1982**, *2*, 226.
(7) Bevilacqua, M.; Alejandre, A. G.; Resini, C.; Casagrande, M.; Ramirez, J.; Busca, G. *Phys. Chem. Chem. Phys.* **2002**, *4*, 4575.
(8) Bevilacqua, M.; Busca, G. *Catal. Commun.* **2002**, *3*, 497.
(9) Marie, O.; Massiani, P.; Thibault-Starzyk, F. *J. Phys. Chem. B* **2004**, *108*, 5073.
(10) Demuth, T.; Hafner, J.; Benco, L.; Toulhoat, H. *J. Phys. Chem. B* **2000**, *104*, 4593.
(11) Bucko, T.; Benco, L.; Demuth, T.; Hafner, J. *J. Chem. Phys.* **2002**, *117*, 7295.
(12) Alberti, A. *Zeolites* **1997**, *19*, 411.
(13) Dominguez-Soria, V. D.; Calaminici, P.; Goursot, A. *J. Chem. Phys.* **2007**, *127*, 154710.
(14) Amoureux, J. P.; Bauer, F.; Ernst, H.; Fernandez, C.; Freude, D.; Michel, D.; Pingel, U. T. *Chem. Phys. Lett.* **1998**, *285*, 10.
(15) Bull, L. M.; Bussemer, B.; Anupold, T.; Reinhold, A.; Samoson, A.; Sauer, J.; Cheetham, A. K.; Dupree, R. *J. Am. Chem. Soc.* **2000**, *122*, 4948.
(16) Bull, L. M.; Cheetham, A. K. *Stud. Surf. Sci. Catal.* **1997**, *105*, 471.
(17) Bull, L. M.; Cheetham, A. K.; Anupold, T.; Reinhold, A.; Samoson, A.; Sauer, J.; Bussemer, B.; Lee, Y.; Gann, S.; Shore, J.; Pines, A.; Dupree, R. *J. Am. Chem. Soc.* **1998**, *120*, 3510.
(18) Freude, D.; Loeser, T.; Michel, D.; Pingel, U.; Prochnow, D. *Solid State Nucl. Magn. Reson.* **2001**, *20*, 46.

(19) Loeser, T.; Freude, D.; Mabande, G. T. P.; Schwieger, W. *Chem. Phys. Lett.* **2003**, *370*, 32.
(20) Neuhoff, P. S.; Shao, P.; Stebbins, J. F. *Microporous Mesoporous Mater.* **2002**, *55*, 239.
(21) Pingel, U. T.; Amoureux, J. P.; Anupold, T.; Bauer, F.; Ernst, H.; Fernandez, C.; Freude, D.; Samoson, A. *Chem. Phys. Lett.* **1998**, *294*, 345.
(22) Readman, J. E.; Kim, N.; Ziliox, M.; Grey, C. P. *Chem. Commun.* **2002**, 2808.
(23) Stebbins, J. F.; Zhao, P. D.; Lee, S. K.; Cheng, X. *Am. Mineral.* **1999**, *84*, 1680.
(24) Peng, L.; Huo, H.; Liu, Y.; Grey, C. P. *J. Am. Chem. Soc.* **2007**, *129*, 335.
(25) Peng, L.; Liu, Y.; Kim, N.; Readman, J. E.; Grey, C. P. *Nat. Mater.* **2005**, *4*, 216.
(26) Kolodziejski, W.; Klinowski, J. *Chem. Rev.* **2002**, *102*, 613.
(27) Haw, J. F.; Richardson, B. R.; Oshiro, I. S.; Lazo, N. D.; Speed, J. A. *J. Am. Chem. Soc.* **1989**, *111*, 2052.
(28) Goetz, J. M.; Wu, J. H.; Yee, H. F.; Schaefer, J. *Solid State Nucl. Magn. Reson.* **1998**, *12*, 87.
(29) Gullion, T. *Magn. Reson. Rev.* **1997**, *17*, 83.
(30) Wu, J. H.; Xiao, C. D.; Yee, A. F.; Goetz, J. M.; Schaefer, J. *Macromolecules* **2000**, *33*, 6849.
(31) Fyfe, C. A.; Mueller, K. T.; Grondey, H.; Wong-Moon, K. C. *J. Phys. Chem.* **1993**, *97*, 13484.
(32) Gullion, T.; Schaefer, J. *J. Magn. Reson.* **1989**, *81*, 196.
(33) Eichele, K. *WSolids ver. 1.17.30*; Universität Tübingen, 2001.
(34) Bak, M.; Rasmussen, J. T.; Nielsen, N. C. *J. Magn. Reson.* **2000**, *147*, 296.
(35) Liu, H. M.; Kao, H. M.; Grey, C. P. *J. Phys. Chem. B* **1999**, *103*, 4786.
(36) Kao, H. M.; Grey, G. P. *J. Phys. Chem.* **1996**, *100*, 5105.
(37) Maache, M.; Janin, A.; Lavalley, J. C.; Benazzi, E. *Zeolites* **1995**, *15*, 507.
(38) Kao, H. M.; Yu, C. Y.; Yeh, M. C. *Microporous Mesoporous Mater.* **2002**, *53*, 1.
(39) Kao, H. M. Probing the Bronsted and Lewis Acid Sites in Zeolite Y with Probe Molecules and Solid-State Double Resonance NMR. Ph.D. Dissertation, State University of New York at Stony Brook, 1998.
(40) Hunger, M. *Solid State Nucl. Magn. Reson.* **1996**, *6*, 1.
(41) Peng, L.; Huo, H.; Gan, Z.; Grey, C. P. *Microporous Mesoporous Mater.* **2008**, *109*, 156.
(42) Czjzek, M.; Jobic, H.; Fitch, A. N.; Vogt, T. *J. Phys. Chem.* **1992**, *96*, 1535.
(43) Vankoningsveld, H.; Jansen, J. C.; Vanbekkum, H. *Zeolites* **1990**, *10*, 235.
(44) Ichikawa, M. *Acta Crystallogr., Sect. B* **1978**, *34*, 2074.
(45) Ichikawa, M. *J. Mol. Struct.* **2000**, *552*, 63.
(46) Kobe, J. M.; Gluszak, T. J.; Dumesic, J. A.; Root, T. W. *J. Phys. Chem.* **1995**, *99*, 5485.
(47) Bankos, I.; Valyon, J.; Kapustin, G. I.; Kallo, D.; Klyachko, A. L.; Brueva, T. R. *Zeolites* **1988**, *8*, 189.
(48) Karge, H. G.; Dondur, V. *J. Phys. Chem.* **1990**, *94*, 765.
(49) Crocker, M.; Herold, R. H. M.; Sonnemans, M. H. W.; Emeis, C. A.; Wilson, A. E.; Vandermoolen, J. N. *J. Phys. Chem.* **1993**, *97*, 432.
(50) Datka, J.; Gil, B.; Kubacka, A. *Zeolites* **1995**, *15*, 501.
(51) Sawa, M.; Niwa, M.; Murakami, Y. *Zeolites* **1990**, *10*, 532.
(52) Alberti, A.; Davoli, P.; Vezzalini, G. *Z. Kristallogr.* **1986**, *175*, 249.
(53) Derouane, E. G.; Fripiat, J. G. Proceedings of the 6th International Zeolite Conference, Guildford, 1983.